GEOPHYSICS, VOL. 57, NO. 5 (MAY 1992); P. 710–719, 11 FIGS., 1 TABLE.

Attenuation mechanisms in sands: Laboratory versus theoretical (Biot) data

Manika Prasad* and Rolf Meissner‡

ABSTRACT

The velocity and attenuation of compressional- (Q_P^{-1}, V_P, respectively) and shear waves (Q_S^{-1}, V_S, respectively), determined with the Pulse Transmission technique at a frequency of about 100 kHz, are compared with the grain size, shape, porosity, density, and static frame compressibility of dry and water-saturated sands. Except for V_S, all the quantities V_P, Q_P^{-1} and Q_S^{-1} are dependent on grain size and are higher in coarser grains than in finer grains. Q_S^{-1} decreases significantly with increasing differential pressure in coarse-grained sediments, but the same sediments show an anomalous increase with differential pressure in Q_P^{-1} at low pressures. We have also modeled the V_P, V_S, Q_P^{-1}, and Q_S^{-1} of these samples to understand the mechanisms governing the observed changes. The Contact Radius model with surface force effects predicts both V_P and V_S to be dependent on grain size. Frictional losses in unconsolidated coarse-grained sands must also be considered at small strains (10^{-7}). Velocity and losses measured in saturated sands are higher than those predicted by the Biot model, which does not account for any grain size dependence of the seismic qualities.

INTRODUCTION

Seismic surveys combining both P- and S-wave information yield more reliable predictions of possible physical parameters. Knowledge about attenuation of P- (Q_P^{-1}) and S- (Q_S^{-1}) waves can help to solve any ambiguity in data interpretation due to overlapping of seismic velocity range of P- (V_P) and S- (V_S) waves for different materials. It is normally accepted that velocities and quality factors increase with pressure. A change in lithology from air-filled to fluid-filled pores leads to a jump in V_P, V_S remaining rather

LIST OF SYMBOLS

Q	quality factor
V	velocity
R	grain size
b	initial contact radius
a	deformed contact radius
Y	normal force
Y^*	effective normal force
D_N	normal stiffness
D_T	tangential stiffness
ξ	surface energy
δ	displacement due to Y^*
K	coordination number
ϕ	porosity
ρ_Q	grain density
ρ_f	pore fluid density
η	pore fluid viscosity
ν	grain poisson's ratio
μ_Q	grain shear modulus
K_Q	grain bulk modulus
K_f	pore fluid bulk modulus
μ^*	effective shear modulus
λ^*	effective lame's constant
K^*	effective bulk modulus
E_S	static frame compressibility
A	arbitrary area
A_C	total area of contact in A
P	hydrostatic pressure
F_S	frictional force due to P
T_S	shear force
V_L	volume
ΔW_C	frictional energy loss per cycle
ΔW	total loss in V_L
W_L	total work done in V_L
ε	shear strain due to transducers
F_η	viscosity correction factor in the Biot model

Manuscript received by the Editor September 27, 1990; revised manuscript received October 18, 1991.
*School of Ocean and Earth Science and Technology, University of Hawaii, 2525 Correa Street, Honolulu, Hawaii 96822.
‡Institut fuer Geophysik, Leibnitzstr 15, 2300 Kiel, Federal Republic of Germany.

unaffected. Small amounts of clay in a sediment result in velocity decreases (Han et al., 1986). Attenuation is very sensitive to the presence of volatiles. With only 1 to 2 percent volatiles, both Q_P and V_P decrease significantly. S-waves remain unaffected by the presence of volatiles (Clark, 1980; Murphy, 1982, 1984; Muckelmann, 1985). From in-situ measurements in marine sediments, Hamilton (1972) reports an increase in attenuation with decreasing grain size. Existing theoretical models of Biot (1956a, b), Gassmann (1951), and the Contact Radius Model (Duffy and Mindlin, 1957; Mindlin, 1949; Mindlin and Deresiewicz, 1953) however, do not suggest any grain size dependence of V and Q^{-1}. Our main aim is to study the effects of grain size, shape, porosity, permeability, pore filling, and static frame compressibility on V_P, V_S, Q_P^{-1}, and Q_S^{-1} under laboratory conditions using samples covering a wide range of grain sizes.

For the measurements of V and Q, a 100 kHz pulse transmission apparatus was constructed at the Institute of Geophysics in Kiel (Muckelmann, 1985). It allows P- and S-wave recordings along with simultaneous measurements of porosity, permeability, and density at different confining pressures. Here we report results of experiments on sand, samples varying from coarse sands to silt grain sizes. These results help us to establish the possibility of a correlation between seismic and geological parameters. We also compare our data with predictions of theoretical models for these samples. The Contact Radius Model (CRM) and the Friction Model (FM) approximate dry samples and the Biot model (BM) is examined for the saturated case.

EXPERIMENTAL PROCEDURE

Sample description

We have examined the grain size, shape, porosity, permeability, static frame compressibility and shear strength of round and angular sands and quartz powders used in the pulse transmission experiments.

All samples taken were very well sorted with less than 1 percent clay content. The uniformity coefficient (Figure 1), a measure of sediment sorting, was less than two. On an average, the porosity of all samples lay between 25 and 40 percent and the permeability was between 1 and 100 darcy. The grain shapes observed under microscope were round and angular. Both static frame compressibility and shear strength displayed grain size and shape dependence. The static frame compressibility from soil consolidation tests is lower in coarse-grained samples. It is also lower in samples with rounded grains. In uniaxial shear tests too, a difference in the angle of inner friction is seen between rounded, angular, and powdered samples. All samples show small values of cohesive strength, which could be due to the capillary action causing an apparent cohesion. A detailed description of the samples is given in Prasad (1988).

Summarizing, we observe that coarser samples have higher permeability and density and lower static frame compressibility and porosity than finer ones. Angular grained samples have higher frame compressibility than similar rounded grained samples.

Seismic Experiments

The seismic experiments were carried out with a pulse transmission apparatus at a frequency of about 100 kHz. Aluminum probes were used to calibrate the transducer setup. In the noise-free data obtained in the laboratory, the two methods of attenuation calculation, rise time and spectrum division, were used, with aluminum as standard reference. The rise time results were calibrated with spectrum division for each configuration of sources and receivers (Muckelmann, 1985).

The seismic experiments, conducted on dry and fully water-saturated samples, also reflect grain size dependence observed in the geo-technical properties. In the following, unless otherwise specified, "saturated" means water saturation.

Dry samples.—The samples were dried at 80°C in the oven. A vacuum of about one atmospheric unit was maintained during experiments. Despite this, the results indicate that some moisture is retained in the samples.

V_P (Figure 2, bottom) is higher in coarse grained samples P1 and P2 than in fine grained samples P5 and P6. It is also higher in similar sized but round grained samples P1 and P6 than in the angular grained samples A1, A4, and H200. V_S (Figure 2, top) is the same for all but one sample. It is lower in the quartz powder H200.

The attenuation in dry samples is higher than or equivalent to that in saturated samples. Q_P^{-1} (Figure 3, bottom) is higher in coarse grained samples P1 and A1 than in fine grained samples P6 and A4. Sample P6 with rounded grains is coarser than angular grained sample A4, but Q_P^{-1} in both is similar. The quartz powder H200 has the highest Q_P^{-1} values. Q_S^{-1} (Figure 3, top) is highest in the quartz powder H200, followed by coarser grained P1. The angular grained samples do not show much difference in their attenuation values. The attenuation in the finer grained angular sample A4 is higher than in the comparatively coarser grained rounded sample P6. Also the gradient of Q_S^{-1} decrease with pressure is higher for the coarser sands and for the quartz powder H200.

Saturated samples.—V_P (Figure 4, bottom) shows higher values in coarser samples than in finer ones and increases with pressure for all samples. The angular sample A2 with higher static frame compressibility shows lower V_P-values than the rounded sample P6 with similar grain size. In contrast to V_P, V_S shows no dependence on grain size and shape (Figure 4, top).

Q_P^{-1} and Q_S^{-1} display strong grain size dependence. Both are higher in coarse-grained samples. Q_P^{-1} (Figure 5, bottom) in coarse-grained samples shows an anomalous behavior with increasing pressure; in samples P1, P2, and P3, Q_P^{-1} seems to increase with pressure. This effect is not seen in the finer grained samples P5 or P6, where Q_P^{-1} remains constant or decreases slightly with pressure. Q_S^{-1} decreases with pressure for all samples (Figure 5, top). The gradient of decrease in Q_S^{-1} with pressure is higher in coarser than in finer sands.

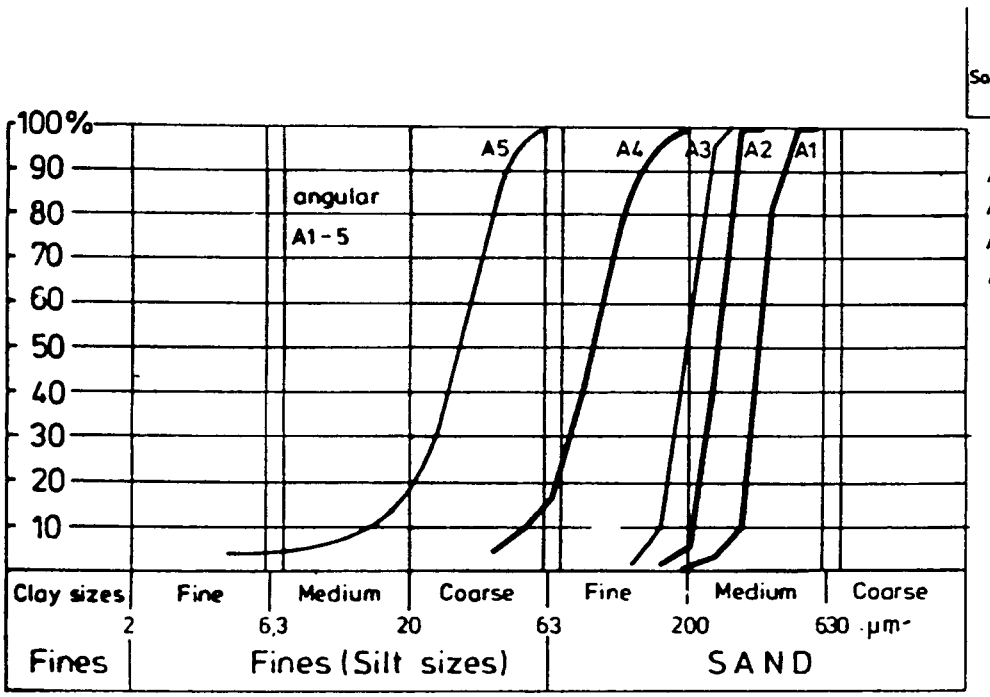

Sample	eff. grain size D 10 µm	Median D 50 µm	U: d60/d10
A1	310	360	1.2
A2	205	255	1.3
A3	160	205	1.3
A4	52	91	1.88
A5	14	30	2.36

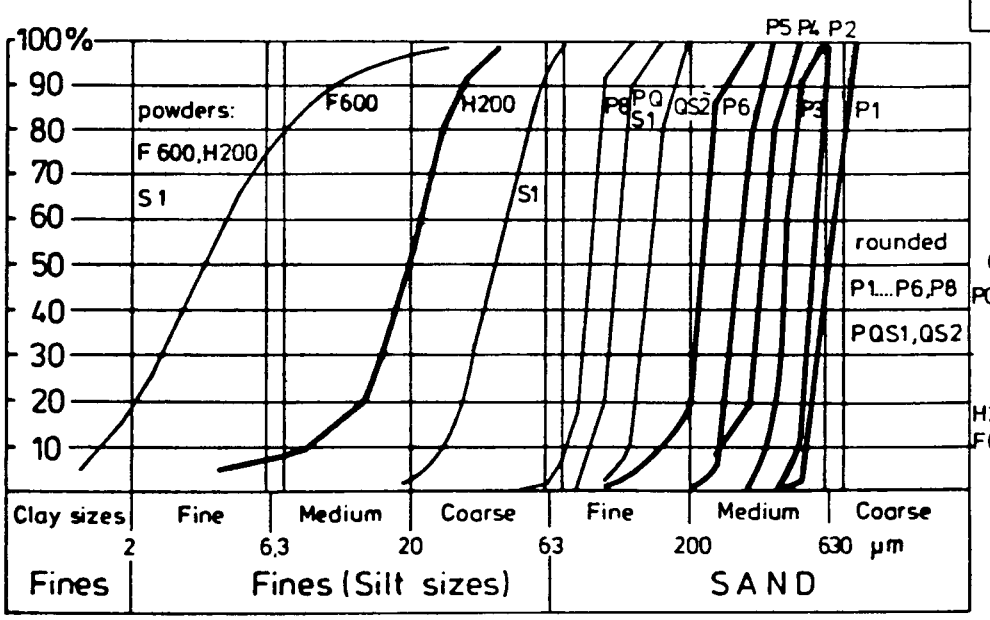

Sample	eff. grain size D 10 µm	Median D 50 µm	U: d60/d10
P1	530	650	1.3
P2	500	550	1.1
P3	380	460	1.2
P4	270	360	1.4
P5	255	300	1.2
P6	160	220	1.4
QS2	120	145	1.25
PQS1	89	110	1.3
P8	74	90	1.2
S1	27	41	1.66
H200	9	20	2.4
F600	1.6	3.7	2.75

FIG. 1. Grain size analysis of the angular (top), rounded and powdered (bottom) samples. Bold curves represent samples measured in the seismic experiment. The uniformity coefficient, its median, and effective grain size are given in the adjoining table.

Loss diagram

To differentiate between bulk and shear losses, the laboratory data for all samples are plotted in a $(V_P/V_S)^2$ versus (Q_P/Q_S) diagram (Figure 6). This relationship was established by Winkler and Nur (1982) and studied again by Meissner and Theilen (1983) for field data and laboratory samples. In this "loss diagram" the samples can be sorted on the basis of their pore filling (water or air) and their grain shapes. The $(V_P/V_S)^2$ ratio is high (10 to 30) in saturated samples, whereas dry samples are marked by low ratios (<10). The lines drawn in Figure 6 for various imaginary bulk K_i to imaginary shear modulus μ_i relationships allow an estimation of the main attenuation mechanisms. The rounded saturated samples are characterized by surprisingly strong bulk losses ($K_i \approx 10\ \mu_i$). The angular saturated samples possibly show higher shear losses ($K_i \approx 5\ \mu_i$), but this should be confirmed by more data points. In dry samples, the losses are about equal in bulk and shear for both, rounded and angular, grain shapes. Only the powdered sample H200 shows higher losses in shear. Here the powdered sample resembles clays, which are characterized by high shear losses making them almost impervious to shear waves at low pressures.

Grain size and frame compressibility dependence

From our observations with different grain sizes, we see a marked grain size dependence of geological and seismic properties. Figures 7 and 8 illustrate the relationship between the compressional modulus, K^* and shear modulus, μ^* obtained from measured values of V_P and V_S. μ^* (Figure 7, top) is not influenced by grain size and, in round grained samples, by pore filling. But it is much lower in dry angular grained samples. In contrast, K^*, in Figure 7 (bottom) for dry samples and in Figure 8 (bottom) for saturated samples, is higher in coarser grained samples. An angular grain shape further reduces K^*. Interestingly, Q_P^{-1} *and* Q_S^{-1} show a grain size dependence; both are higher in coarse grained samples.

We notice a certain correlation between V_P and the static frame compressibility E_S. In Figure 9, V_P is plotted against static frame compressibility E_S for all saturated samples. At low pressures, marked by low V_P and E_S values, there is almost a linear relationship. At higher pressures (high V_P and E_S) the values separate with higher V_P for rounded coarse grained samples P1 and P2 and lower values for fine grained and for angular samples of similar size. The linear relationship could imply that, at lower pressures compaction is a major governing factor for V_P. It increases with increasing compaction. Since fine grains do not show much change in compaction, these samples (P6) separate from the linear relationship, implying that no major change takes place with compaction. The coarse grains are compacted to a higher degree and so E_S influences V_P to a greater extent. Other governing factors enter into play later here.

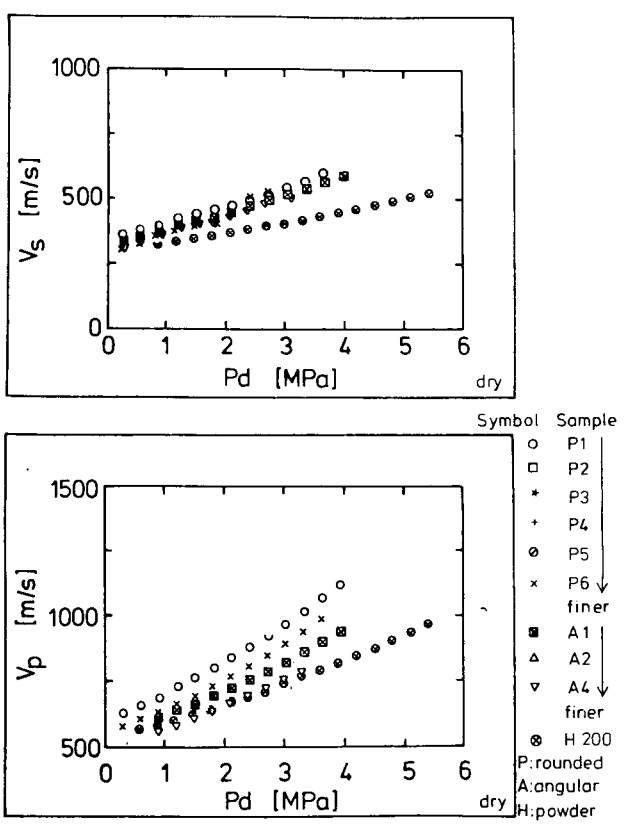

FIG. 2. V_P (bottom) and V_S (top) in dry samples. V_P is higher in coarser grains. V_S is unaffected by grain size.

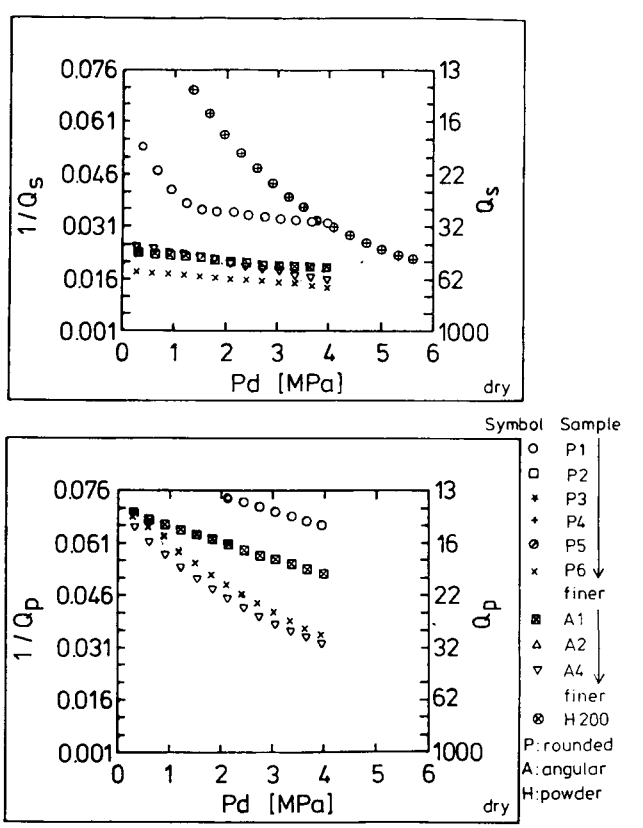

FIG. 3. Q_P^{-1} (bottom) and Q_S^{-1} (top) in dry samples. Both Q_P^{-1} and Q_S^{-1} are higher in the coarser samples.

THEORETICAL MODELS

We now examine the Contact Radius Model (CRM), Friction Model (FM), and Biot Model (BM) to approximate our measurements in dry and saturated samples. The frame parameters and V_P and V_S are modeled with the CRM which relates a change in contact radius between grains of a sample to its elastic moduli. The BM (Biot, 1956a and b, 1962, 1973) predictions on the basis of global flow losses due to relative movement between pore fluid and frame are compared to experimental observations of V_P, V_S, Q_P^{-1}, and Q_S^{-1} in saturated sediments. Frictional losses in the frame are considered by the FM.

Contact radius model (CRM)

At its simplest, the CRM considers two elastic, homogeneous, identical spherical particles in contact. The radius of the area of contact between the spheres increases upon deformation due to a normal force. On application of a force Y, the normal (D_N) and tangential (D_T) stiffness of a sample with uniform grain size R and initial contact radius b are given by Duffy and Mindlin (1957) as

$$D_N = 2\mu_Q a/(1 - \nu)$$

and

$$D_T = 4\mu_Q b/(2 - \nu). \quad (1)$$

We use the equations of Digby (1981) for the relationship between a normal force Y and the relative displacement δ of the centers of the spheres:

$$Y = \frac{4\mu_Q}{1 - \nu}\left[a\delta - \frac{(a^2 - b^2)^{1.5}}{3R}\right], \quad (2)$$

where

$$\delta = a\sqrt{a^2 - b^2}/R. \quad (3)$$

Additional surface effects observed as apparent cohesion in shear tests on sands enhance this force. Johnson et al. (1971) relate the cohesive strength to surface energy per unit area ξ of the elastic bodies through the action of surface forces. With this modified force Y^* given by them as

$$Y^* = Y + 3\xi\pi R + \sqrt{6\xi\pi RY + (3\xi\pi R)^2}, \quad (4)$$

the deformed contact radius a is calculated from equations (2), (3), and (4). Results of calculations for different grain sizes and initial contact radii (Figure 10 a–d, a finest, d coarsest) show that:

1) at small pressures, there is an abrupt increase in the contact radius. This increase is much larger for coarser grains (Figure 10d),
2) the contact radius tends towards a limiting value beyond which there is little change with pressure. The

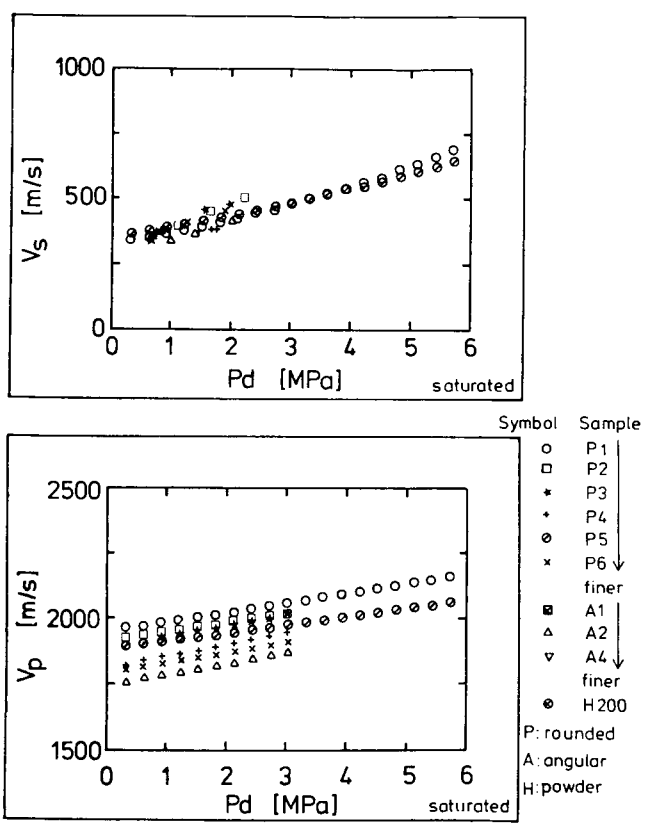

FIG. 4. V_P (bottom) and V_S (top) in saturated samples. V_P shows clear grain size dependence, also the angular sample has least V_P. V_S is unaffected by grain size.

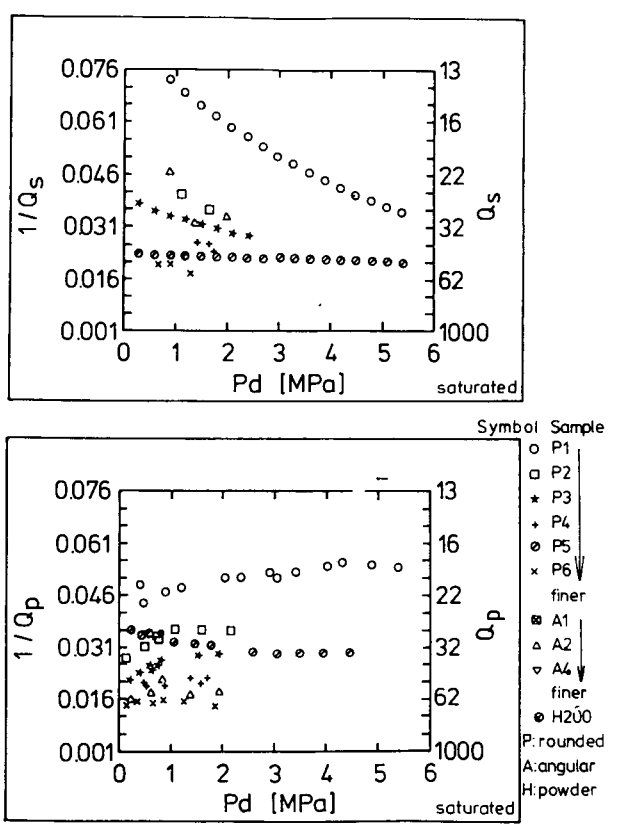

FIG. 5. Q_P^{-1} (bottom) and Q_S^{-1} (top) in saturated samples. The coarse grains show higher attenuation values. Q_P^{-1} in coarse samples P1, P2, and P3 shows slight increase at low pressure, which is not seen in finer samples P4, P5, and P6.

limiting contact radius is arrived at much lower pressures for finer grains (Figure 10a).

Assuming an initial contact radius between loose grains due to apparent cohesion, the equations of Digby (1981) for the effective moduli μ^*, λ^*, and K^* can be expressed as:

$$2\mu^* = \frac{\mu_Q K(1-\phi)}{5\pi R}\left[\frac{a}{1-\nu} + \frac{3b}{2-\nu}\right], \quad (5)$$

$$\lambda^* = \frac{\mu_Q K(1-\phi)}{5\pi R}\left[\frac{a}{2(1-\nu)} - \frac{b}{2-\nu}\right], \quad (6)$$

$$K^* = \frac{\mu_Q K(1-\phi)}{5\pi R}\left[\frac{5a}{6(1-\nu)}\right]. \quad (7)$$

μ^* and K^* calculated with equations (5) and (7) are plotted in Figure 7 (top and bottom, resp.) along with the measured values. Porosity and effective pressure values are taken from the P.T. experiments. Other physical parameters are given in

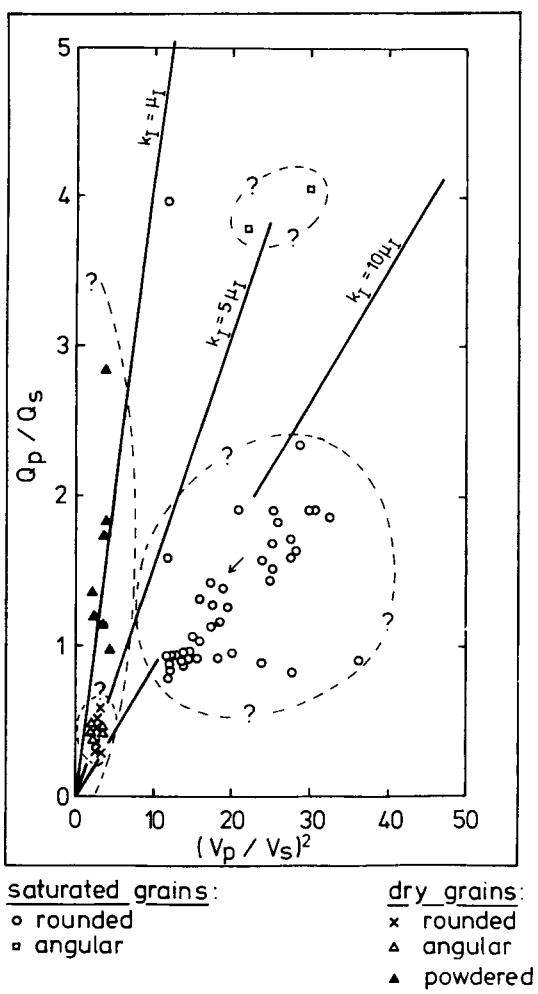

FIG. 6. (Q_P/Q_S)-$(V_P/V_S)^2$ relationship for all samples. Arrows give direction of pressure decrease, broken lines delineate possible loss mechanisms for the different sediment types. Solid lines give the relationships between the imaginary shear and bulk moduli (μ^* and K^*, respectively).

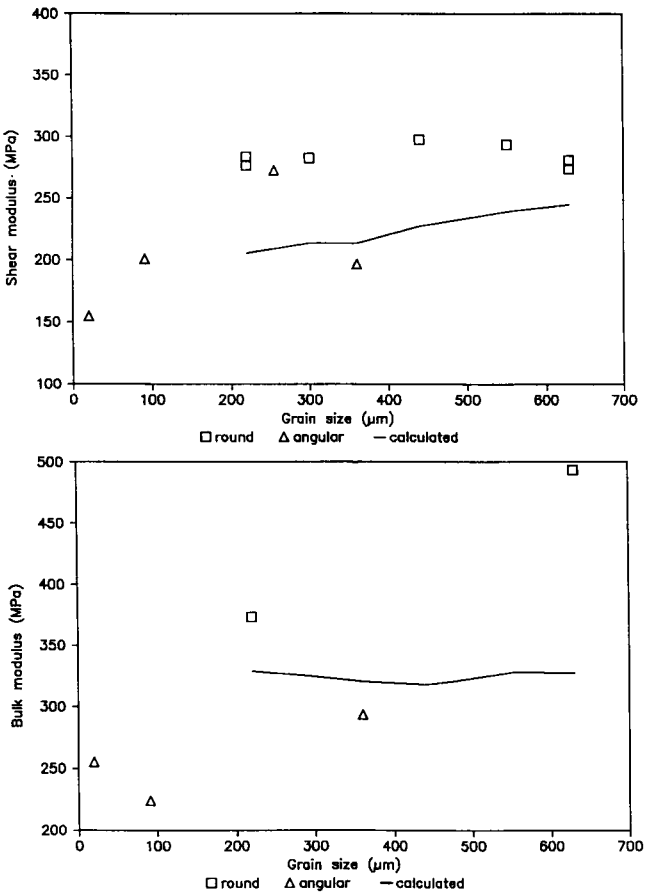

FIG. 7. K^* (bottom) and μ^* (top) as a function of grain size. Solid lines mark values predicted by the CRM at $b = 0$ μm. Measured values are denoted by symbols.

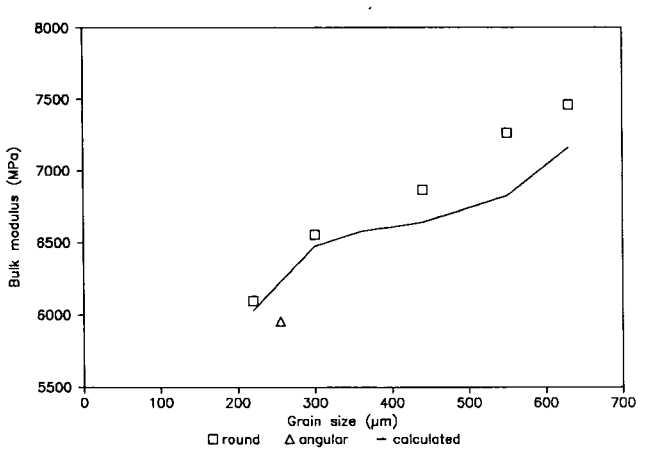

FIG. 8. K^* as a function of grain size in saturated samples. Solid lines mark values predicted by the BM. Measured values are denoted by symbols.

Table 1. The calculations for no initial contact radius ($b = 0$) does not predict any grain size dependence of both moduli. A grain size dependence enters the model with varying initial contact radius. But this predicts a grain size dependence of μ^* as well, which is contrary to our observations. The calculated values for μ^* and K^* with $b = 0$ are also somewhat lower than the measured values (Figure 7).

Friction model (FM)

Winkler and Nur (1982) and Stewart et al. (1983) report that frictional losses at strains $<10^{-6}$ are negligible in rock samples. To estimate the effects of strain in terrain with a weathering layer or with unconsolidated sediments, we evaluate frictional losses for this loose packing of sand grains from frictional and shear forces acting on each grain. The work lost at the contacts compared with the total work done gives a measure of the attenuation due to friction.

The total area of contact A_C in an arbitrary area A can be derived from an estimation of the number of contacts in it (Prasad, 1988). The normal force in this area of contact due to a hydrostatic pressure P is given by

$$Y^* = 3Kb^2(1 - \phi)(0.5\pi^2 - 2)P/32\pi R^2. \quad (8)$$

At each contact area the frictional force F_S due to this normal force is juxtaposed to shear force T_S due to the transducer strain ε, where

$$T_S = \frac{K\mu^*(1 - \Phi)}{5\pi R}\left[\frac{3b}{2 - \nu} + \frac{a}{1 - \nu}\right] A_C\varepsilon. \quad (9)$$

Putting the two, frictional and shear, forces in relation gives the losses at the contacts. According to Mindlin and Deresiewicz (1953), for a constant normal force Y^* and an oscillating tangential force T_S, the frictional energy loss per cycle ΔW_C for one contact area can be given by

$$\Delta W_C = (2 - \nu)T_S^3/36\mu_Q aF_S. \quad (10)$$

In this formulation, T_S is smaller than F_S, else the grains tend to shear across each other. Taking the total loss ΔW in volume V_L containing spheres with K number of contacts per sphere as:

$$\Delta W = \frac{(2 - \nu)T_S^3}{36\mu_Q aF_S}\frac{3K}{4\pi R^3}V_L, \quad (11)$$

the total work W_L done in volume V_L given by

$$W_L = 0.5V_L\mu^*\varepsilon^2 \quad (12)$$

and attenuation Q^{-1} given by

$$Q^{-1} = \Delta W/2\pi W_L \quad (13)$$

(Stewart et al., 1983), we get an expression for Q_S^{-1}

$$Q_S^{-1} = \frac{(2 - \nu)K^4}{6000\mu_Q\pi^4R^6}\frac{\mu^{*2}(1 - \phi)^3A_C^3\varepsilon}{aF_S}\left[\frac{3b}{2 - \nu} + \frac{a}{1 - \nu}\right]^3, \quad (14)$$

which is dependent on the grain size R, compaction b and shear strain ε (Prasad, 1988). We now examine the effect of strain by assuming $\varepsilon \approx 10^{-6}$ (Figure 11, top) and $\varepsilon \approx 10^{-7}$ (Figure 11, bottom) in equation (15) for different grain sizes. In both cases, the losses are grain size dependent. Attenua-

Table 1. Values of physical properties used in the numerical computations.

μ_Q	= 36.5 GPa
K_f	= 2.22 GPa
K_Q	= 51.2 GPa
η	= 0.001 kg/ms
K	= 9
ρ_f	= 997.1 kg/m^3
ρ_Q	= 2650.0 kg/m^3
ν	= 0.2

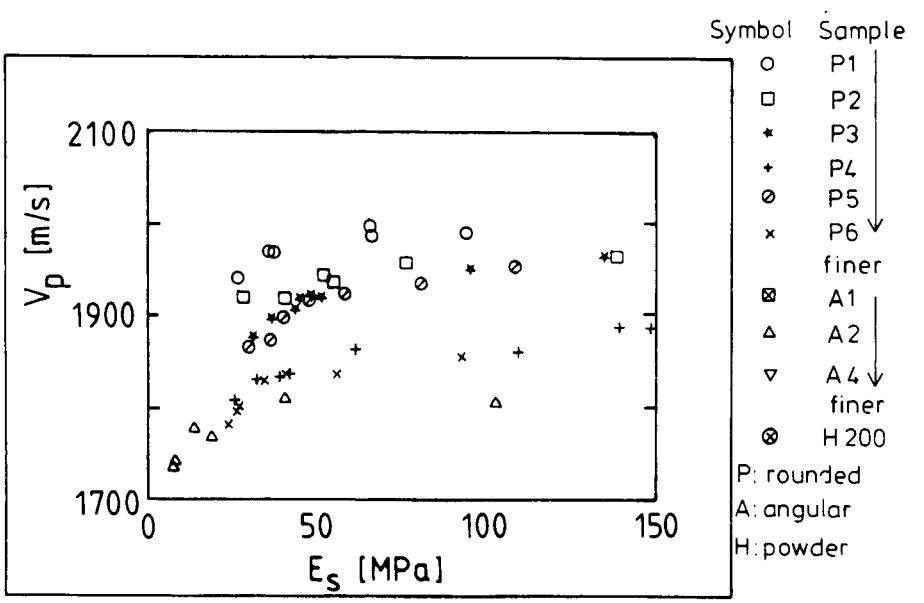

FIG. 9. E_S-V_P relationship in saturated samples. At low pressure a certain relationship between E_S and V_P seems to exist.

tion is high for coarse grains and decreases rapidly with pressure. In finer grains attenuation is low and decreases only slightly with pressure. Also at $\varepsilon \approx 10^{-7}$ coarse sands do show considerable losses. This bears a grave consequence for seismic studies especially near a seismic source, where such strains can occur, and must also be considered in planning seismic surveys.

Biot model (BM)

The frame moduli derived from the CRM are substituted in the BM to model the saturated case. BM describes wave propagation in a two phase system, a porous elastic frame and a viscous, incompressible pore fluid. The losses are ascribed to relative motion between the frame and its pore fluid. We use the complex frequency dependent viscosity correction factor F_η suggested by Biot to model our high frequency experiments. Attention is devoted to the P-wave of the "first kind." The "second kind" of P-wave (Biot, 1956a, and b) is largely diffusive at the frequency of measurement (about 100 kHz) with velocity about 200 to 300 m/s. K^*-values predicted by the BM (Figure 8) are lower than those measured in the laboratory. A grain size dependence of velocity enters the model mainly through permeability which is strongly dependent on grain size distribution of the sample.

DISCUSSION

The results of our measurements on a broad range of grain sizes and other geological properties are useful in relating them to characteristics of seismic layers in the field and for an interactive in-situ study of sediments with respect to physical and seismic properties. They are also important to understand the mechanisms of seismic wave propagation and attenuation in sediments.

A comparison between our observations and the theoretical models discussed earlier allows an evaluation of prevalent loss mechanisms. The Q_S^{-1} results (Figure 5, top) show significant similarity to the contact radius calculations with the CRM for different grain sizes (Figure 10). In coarser grains the increase in contact radius (Figure 10d) and de-

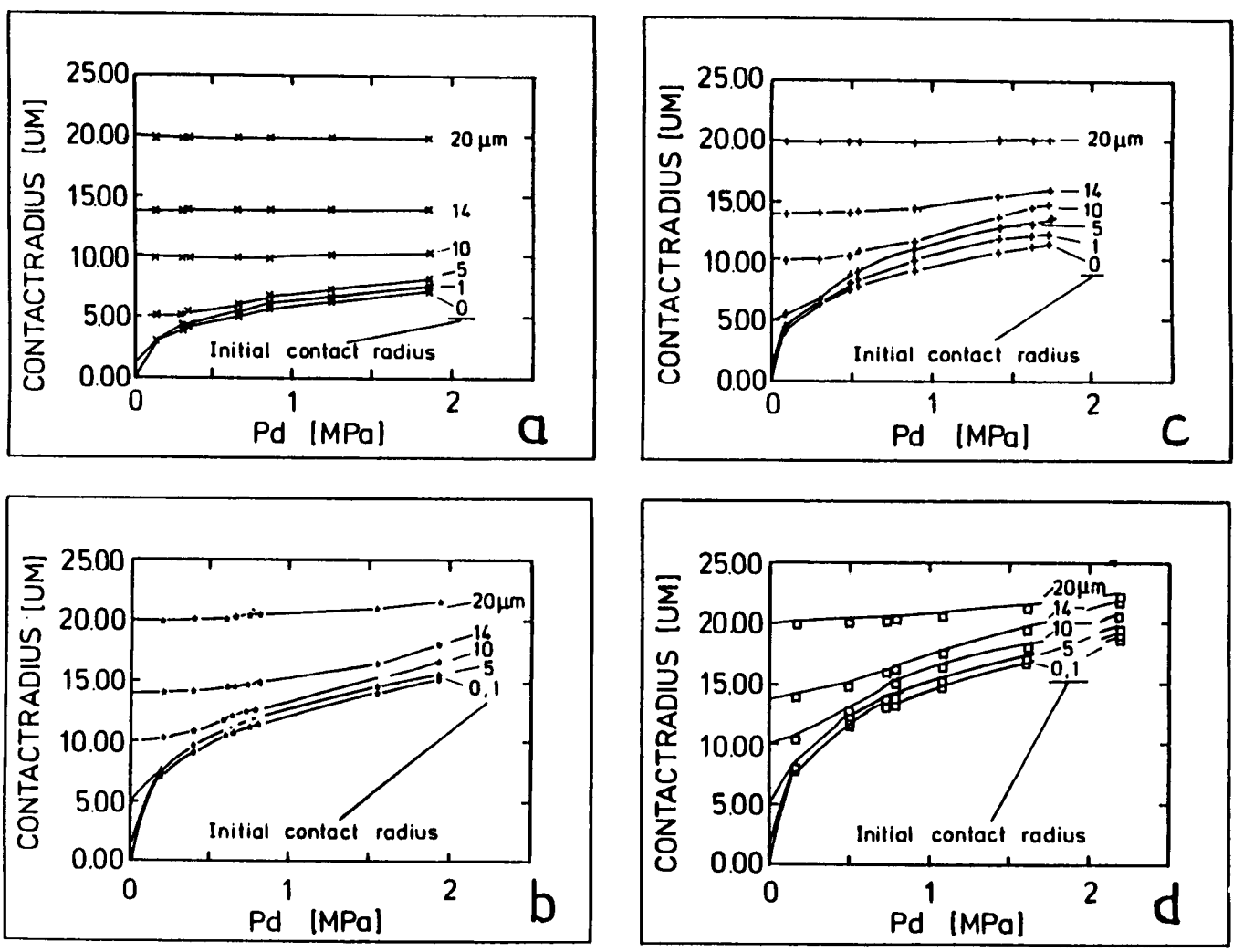

FIG. 10. Change in contact radius with pressure for different grain sizes. (a) R = 110 µm, (b) R = 150 µm, (c) R = 225 µm, (d) R = 275 µm. The number on each curve denotes initial contact radius taken for its calculation.

crease in Q_S^{-1} (Figure 5, top, samples P1 and P2) is much higher at lower pressures. Finer grains do not show much change in contact radius (Figure 10a) and Q_S^{-1} with pressure (Figure 5, samples P5 and P6). If attenuation in unconsolidated sediments is considered to be due to a loose packing of the grains and relative motion between them, seismic energy being lost in friction, the attenuation characteristics of different grain sizes is explainable on the basis of their distinct contact radius changes. An increase in pressure leads to an increase in contact radius, a denser packing, and, with it, higher shear strength. The stable packing of the finer grains due to their own weights prevents any predominant relative motion between grains, and so attenuation change with pressure is not so pronounced as opposed to the coarser grains which show considerable displacement and readjustment with pressure. The elastic moduli calculated with the model assuming no initial contact radius ($b = 0$) show no grain size dependence and are lower than the measured values. On introduction of an initial contact radius, both μ^* and K^* show a grain size dependence. But, since we have not considered attenuation effects here, and the CRM assumes a Hooke's stress-strain relationship, reformulating it

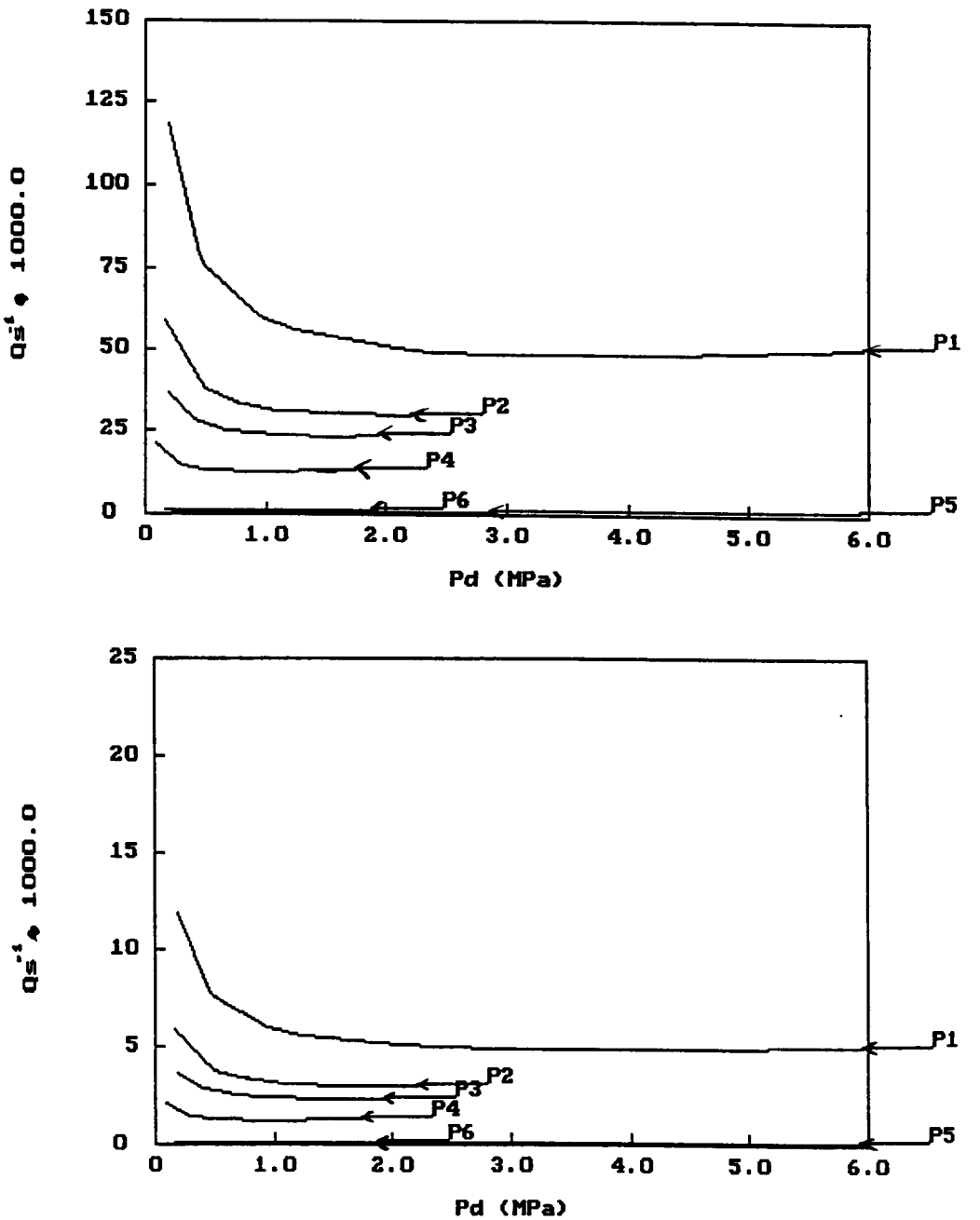

FIG. 11. Frictional attenuation calculated for different grain sizes at $\varepsilon \approx 10^{-6}$ (top) and $\varepsilon \approx 10^{-7}$ (bottom). The coarser grains have higher losses and steeper gradients of decrease with pressure. At $\varepsilon \approx 10^{-7}$ there are still some losses to be expected in coarser grains.

with a different stress-strain relationship would probably relate better with the experiments.

Frictional losses calculated for a loose sand sample are also quite high. Coarse sands are also sensitive to strains $<10^{-7}$. The losses are grain size dependent and display similar characteristics as those measured: Q_S^{-1} in coarse sands is higher and decreases very sharply with pressure. Finer sands are not as sensitive to pressure. No losses are predicted in them at strains $<10^{-7}$. Comparing this with the results of Stewart et al. (1983) and Winkler and Nur (1982), we see that unconsolidated sands are more sensitive to strain than sandstones which have negligible losses at strains $<10^{-6}$. Since, in seismic surveys, unconsolidated sediments are more likely to be found near the surface, i.e., near the source, the effects of higher strain must be considered. Finally the Biot model is tested for saturated sands using frame moduli calculated with the CRM and losses calculated with the FM. Although the predictions are similar to those measured, they are lower. This has also been reported by various authors, e.g., Bourbie et al. (1987) and Winkler (1985, 1986).

These considerations lead us to advocate the necessity of constructing a model of a sediment, which calculates the frame moduli along with frame losses. These complex moduli can be taken for predictions of the moduli in a saturated sample with due attention given to the various loss mechanisms due to differential movement between pore fluid and frame. Since grain size is seen to influence both velocity and attenuation, and the present models consider this effect only indirectly through porosity and permeability, we need a more direct and rigorous consideration of grain size effects.

CONCLUSIONS

The relationship between geological and seismic parameters observed in this study can be summarized as follows:

1) Static frame compressibility and P-wave velocities correlate with each other at low pressures. This correlation diminishes with increasing pressures.
2) Coarseness of grains increases the velocity and attenuation of P-waves and the attenuation of S-waves. The S-wave velocity is unaffected by grain size.
3) Angularity of grains causes a decrease in velocity and attenuation and an increase in static frame compressibility.
4) Dry grains show high shear losses, whereas saturated grains have predominant bulk losses of seismic energy.

At present, none of the available theories alone explains our observations. A combination of the Contact Radius Model (CRM), Friction Model (FM) and the Biot Model (BM) may be able to explain most of the experimental results on V_P, V_S, Q_P^{-1}, and Q_S^{-1} for a variety of parameters. CRM allows us to calculate frame parameters. With a combination of CRM and BM, we have reduced the unknown parameters in the BM. The addition of FM to CRM and BM incorporates friction losses also. Friction effects remain amplitude dependent, but they are effective at low strain values also in loose sands. This implies that in planning seismic surveys these nonlinear processes must be taken into consideration. They may predominate in unconsolidated sediments near the surface where the seismic source and receivers are located. In saturated sands, losses additional to those described by the Biot model must be considered.

ACKNOWLEDGMENTS

This work was carried out at the University of Kiel where Prasad spent some years working on doctorate research. It was financed by the German Association for Mineraloil and Coal Research (DGMK) under the project "Absorption of Seismic Waves." We thank them for their cooperation. Thanks are also due to Drs. F. Theilen and R. Muckelmann for many fruitful discussions and helpful suggestions.

REFERENCES

Biot, M. A., 1956a, Theory of propagation of elastic waves in fluid saturated porous solids. I: Low frequency range: J. Acoust. Soc. Am., **28**, 168–178.
——— 1956b, Theory of propagation of elastic waves in fluid saturated porous solids. II: High frequency range: J. Acoust. Soc. Am., **28**, 179–191.
——— 1962, Generalised theory of acoustic propagation in porous dissipative media: J. Acoust. Soc. Am., **34**, 1254–1264.
——— 1973, Nonlinear and semilinear rheology of porous solids: J. Geophys. Res., **78**, 4924–4937.
Bourbie, T., Coussy, O., and Zinszner, B., 1987, Acoustics of porous media: Editions Technip, Paris.
Clark, V. A., Spencer, T. W., Tittmann, B. R., Ahlberg, L. A., and Coombe, L. T., 1980, Effects of volatiles on attenuation (Q^{-1}) and velocity in sedimentary rocks: J. Geophys. Res., **85**, 5190–5198.
Digby, P. J., 1981, The effective elastic moduli of porous granular rocks: J. Appl. Mech., ASME, **48**, 803–808.
Duffy, J., and Mindlin, R. D., 1957, Stress-strain relations and vibrations of a granular medium: J. Appl. Mech., ASME, **24**, 585–593.
Gassmann, F., 1951, Ueber die Elastizitaet poroeser Medien: Vierteljahresschrift der Naturforschenden Gesellschaft, Zuerich, **96**.
Hamilton, E. L., 1972, Compressional-wave attenuation in marine sediments: Geophysics, **37**, 620–646.
Han, De-hua, Nur, A., and Morgan, D., 1986, Effects of porosity and clay content on wave velocities in sandstones: Geophysics, **51**, 2093–2107.
Johnson, K. L., Kendall, K., and Roberts, A. D., 1971, Surface energy and the contact of elastic solids: Proc. Roy. Soc. London, **A 324**, 301–313.
Meissner, R., and Theilen, F., 1983, Attenuation of seismic waves in sediments: Proc. 11th World Petroleum Congress, **2**, 363–379.
Mindlin, R. D., 1949, Compliance of elastic bodies in contact: J. Appl. Mech., Trans. ASME, **19**, 259–268.
Mindlin, R. D., and Deresiewicz, H., 1953, Elastic spheres in contact under varying oblique forces: J. Appl. Mech., ASME, **20**, 327–344.
Muckelmann, R., 1985, Theoretische und experimentelle Untersuchungen von P- und S-Wellen in Sanden unter besonderer Beruecksichtigung ihrer Daempfungseigenschaften: Ph.D. thesis, University of Kiel.
Murphy, W. F., 1982, Effects of partial water saturation on attenuation in Massilon sandstone and Vycor porous glass: J. Acoust. Soc. Amer., **71**, 1458–1468.
——— 1984, Acoustic measures of partial gas saturation in tight sandstones: J. Geophys. Res., **89**, 11 549–11 559.
Murphy, W. F., Winkler, K. W., and Kleinberg, R. L., 1986, Acoustic relaxation in sedimentary rocks: Dependance on grain contacts and fluid saturation: Geophysics, **51**, 757–766.
Prasad, M., 1988, Experimental and theoretical considerations of attenuation and velocity interactions with physical parameters in sands: Ph.D. Thesis, University of Kiel.
Stewart, R. D., Toksöz, M. N., and Timur, A., 1983, Strain dependant attenuation observations and a proposed mechanism: J. Geophys. Res., **88**, 546–554.
Winkler, K. W., 1985, Dispersion analysis of velocity and attenuation in Berea sandstone: J. Geophys. Res., **90**, 6793–6800.
——— 1986, Estimates of velocity dispersion between seismic and ultrasonic frequencies: Geophysics, **51**, 183–189.
Winkler, K. W., and Nur, A., 1982, Seismic attenuation: effects of pore fluid and frictional sliding: Geophysics, **47**, 1–15.